

Facilitating Atom Probe Tomography of 2D MXene Films by In Situ Sputtering

Mathias Krämer ^{1,*}, Bar Favelukis², Maxim Sokol², Brian A. Rosen², Noam Eliaz², Se-Ho Kim^{1,3}, and Baptiste Gault ^{1,4,*}

¹Max-Planck-Institut für Eisenforschung, Max-Planck-Straße 1, 40237 Düsseldorf, Germany

²Department of Materials Science and Engineering, Tel Aviv University, P.O.B 39040, Ramat Aviv 6997801, Israel

³Department of Materials Science and Engineering, Korea University, Seoul 02841, Republic of Korea

⁴Department of Materials, Royal School of Mines, Imperial College London, London, SW7 2AZ, United Kingdom

*Corresponding authors: m.kraemer@mpie.de, b.gault@mpie.de

Abstract

2D materials are emerging as promising nanomaterials for applications in energy storage and catalysis. In the wet chemical synthesis of MXenes, these 2D transition metal carbides and nitrides are terminated with a variety of functional groups, and cations such as Li^+ are often used to intercalate into the structure to obtain exfoliated nanosheets. Given the various elements involved in their synthesis, it is crucial to determine the detailed chemical composition of the final product, in order to better assess and understand the relationships between composition and properties of these materials. To facilitate atom probe tomography analysis of these materials, a revised specimen preparation method is presented in this study. A colloidal $\text{Ti}_3\text{C}_2\text{T}_z$ MXene solution was processed into an additive-free free-standing film and specimens were prepared using a dual beam scanning electron microscope / focused ion beam. To mechanically stabilize the fragile specimens, they were coated using an *in situ* sputtering technique. As various 2D material inks can be processed into such free-standing films, the presented approach is pivotal for enabling atom probe analysis of other 2D materials.

Keywords

atom probe tomography, focused ion beam, *in situ* coating, 2D materials, MXenes

Introduction

Since the groundbreaking experimental observation of graphene (Novoselov et al. 2004), there has been significant interest in 2D materials and their fascinating functional properties. Following graphene, the successful synthesis of other 2D elemental materials (Mannix et al. 2017), 2D transition metal dichalcogenides (Manzeli et al. 2017) and 2D perovskites (Lan et al. 2019), to name a few, has significantly expanded the landscape of 2D materials. Because 2D materials have a thickness of one up to a few atomic layers, and thus a high surface-to-volume ratio, they are particularly interesting for applications involving highly surface-active chemical processes, such as energy storage or catalysis (Nicolosi et al. 2013).

MXenes, 2D transition metal carbides and nitrides, have also been the subject of intense research since their discovery by the Barsoum and Gogotsi groups (Naguib et al. 2011). To date, more than 50 different compositions have been synthesized, not even considering the different and highly variable surface chemistries (Anasori et al. 2023; VahidMohammadi et al. 2021). Their top-down synthesis involves two steps, namely the harsh selective etching of the A layer (typically Al, Si or Ga) from a bulk MAX phase(-like) precursor in a typically HF-based wet chemical environment, and the subsequent exfoliation of the obtained weakly bonded multilayer MXenes into individual nanosheets by intercalation of cations or molecules (Alhabeab et al. 2017; Lim et al. 2022). The general chemical formula of MXenes is written as $M_{n+1}X_nT_z$, characterized by $n + 1$ atomic layers of one or more early transition metals M and n interleaved atomic layers of C and/or N, denoted as X, where T_z represents surface termination groups saturating the bare surface during synthesis. Because this synthesis process is scalable (Shuck et al. 2020), and the MXene nanosheets can be easily processed into free-standing films (J. Zhang et al. 2020) or printable inks (C. Zhang et al. 2019), they are attractive and accessible for industrial applications.

The obtained properties are significantly influenced by the detailed synthesis parameters (Thakur et al. 2023), which control in particular the flake size, defect density and surface chemistry. A carefully optimized synthesis route can therefore be used to fine-tune the properties of the MXenes, which is comparable to defect engineering in bulk materials (X. Li et al. 2017). However, Shuck pointed out that MXenes are unfortunately often treated as chemicals rather than materials, because the detailed synthesis route is overlooked (Shuck 2023). For example, in many synthesis protocols for $Ti_3C_2T_z$, the most studied MXene to date, spontaneous intercalation of Li cations (Lukatskaya et al. 2013) is crucial for obtaining large and high-quality, i.e. less defective, monolayer MXene flakes (Ghidiu et al. 2014; Lipatov et al. 2016; Sang et al. 2016; Shekhirev et al. 2022). Although it is known that the presence of Li influences the properties of the MXenes (Chen et al. 2020), it remains a difficult task to localize and quantify Li in the material using the commonly applied techniques (Shekhirev et al. 2021).

Atom Probe Tomography (APT) is an analytical characterization technique with sensitivity to both light and heavy elements and sufficient spatial resolution to address these unanswered questions (Gault et al. 2021). Briefly summarized, the atom probe is a time-of-flight mass spectrometer equipped with a position-sensitive detector, where

individual atomic or molecular ions are field evaporated from the apex of a sharp, needle-shaped specimen. In combination, the recorded time-of-flight and the impact coordinates of the ions on the detector, allow compositional mapping with a sub-nanometer spatial resolution in 3D (De Geuser et al. 2020). Given these capabilities, APT has been increasingly used in recent years to characterize functional nanomaterials, such as nanoparticles for catalysis, as it provides unique compositional insights that enable an understanding of the activity and degradation of these materials (T. Li et al. 2022).

A critical step towards the APT analysis of nanostructures, including nanoparticles, nanosheets and nanowires, was the development of appropriate specimen preparation approaches, as these materials, unlike bulk materials, do not allow straightforward traditional protocols to prepare needle-shaped specimens (Felfer et al. 2015). Common workarounds include the deposition of nanoparticles on pre-sharpened needles by electrophoresis (Tedsree et al. 2011), or the fixation of nanoparticles with a micromanipulator and subsequent coating on a support (Devaraj et al. 2015) followed by sharpening by focused ion beam (FIB) milling. Attachment on pre-sharpened needles combined with a coating has also been proposed (Josten et al. 2022). The deposition of a dense matrix material encapsulating the nanoparticles by atomic layer deposition (Larson et al. 2015) or metallic electrodeposition (Kim et al. 2018) enables the utilization of the commonly used specimen preparation using a dual beam scanning electron microscope (SEM)-FIB (Thompson et al. 2007). In the case of nanowires, their needle-like shape may even allow them to be analyzed without special specimen preparation in an atom probe with a local electrode (Du et al. 2013; Perea et al. 2006).

Despite the wide range of compositions available, and the increasing intensity of research on nanostructures, 2D materials such as MXenes have rarely been investigated using APT. Although graphene is occasionally used to coat biological or liquid APT specimens (Adineh et al. 2018; Qiu et al. 2020a,b,c), the analysis of graphene is only incidental. Previous studies have shown how APT can advance our understanding on the detailed composition of 2D materials, such as the incorporation of impurity elements during the wet chemical synthesis of 2D MoS₂ (Kim et al. 2020), or the influence of alkali elements from synthesis on the oxidation of Ti₃C₂T_z MXenes (Krämer et al. n.d.). In both cases, the nanosheets were embedded in a metallic matrix, but they are very difficult to localize for targeted sample preparation, and the small number of nanosheets in an average data set limits the statistics.

Here, APT analysis is performed by taking advantage of the possibility to process MXenes into free-standing films, i.e. a macroscopic stack of nanosheets with the same orientation held together by weak intermolecular forces such as van der Waals forces or hydrogen bonds. APT specimens of a free-standing Ti₃C₂T_z MXene film were prepared by FIB lift-out. Following sharpening, APT specimens were coated *in situ* by ion milling a Cr lamella as sputter target (Woods et al. 2023), to mechanically stabilize the fragile specimens. In addition to enhanced yield, performance, and increased field-of-view (Schwarz et al. 2023), as well as the reduction of artifacts in the analysis of Li-containing materials (Singh et al. n.d.), the presented workflow involving the *in situ* coating technique may also be a starting point for a simplified and straightforward APT analysis of 2D materials.

Materials and Methods

Synthesis of Ti_3AlC_2 MAX Phase

Ti_3AlC_2 MAX phase was synthesized by solid-liquid reaction. Briefly, TiC (99.5 %, Alfa Aesar), Ti (99.7 %, Strem) and Al (99.7 %, Strem) powders were ball milled at 1800 rpm for a duration of 5 min. The resulting powder mixture was cold pressed and then heat treated in a furnace at 1500 °C for a period of 120 min under a protective Ar environment. Finally, the sintered Ti_3AlC_2 MAX phase was ball milled at 1800 rpm for 5 min to a fine powder, ready for MXene synthesis.

Synthesis of $\text{Ti}_3\text{C}_2\text{T}_z$ MXenes

For $\text{Ti}_3\text{C}_2\text{T}_z$ MXene synthesis, 0.5 g LiF (99 %, Strem) was dissolved in 5 mL 10.2 mol L⁻¹ concentrated HCl (32 %, Bio-Lab) in a high density polyethylene vial, to prepare the etchant for selective etching of the Al layer from the previous sintered Ti_3AlC_2 MAX phase. Etching was done by slowly adding 0.5 g of the MAX phase powder to the solution under constant stirring with a magnetic stirrer at 45 °C degrees for 24 h.

After etching, the complete solution was transferred to a 50 mL centrifuge tube and filled with deionized water (conductivity 0.055 $\mu\text{S cm}^{-1}$). The solution was shaken thoroughly and then centrifuged at 3500 rpm for a duration of 2 min. The supernatant was decanted, and the remaining sediment was replenished with deionized water, shaken and centrifuged again. Washing was repeated several times until the solution reached a near-neutral pH value, i.e. greater than 6. After washing, the tube containing the sediment was refilled with deionized water and the solution was sonicated in an ice bath for 60 min to prevent heating. To remove unetched residues of the MAX phase, the solution was centrifuged at 3500 rpm for 30 min and the black colloidal supernatant containing single layer MXenes was collected. Finally, the colloidal solution with a yield of about 7 g L⁻¹ was stored at 5 °C.

Preparing Free-Standing $\text{Ti}_3\text{C}_2\text{T}_z$ MXene Film

The free-standing MXene film was prepared by vacuum filtration. 5 mL of the colloidal solution was poured into a vacuum filtration system using a Celgard® 3501 membrane. After filtration, the film was removed from the membrane. Figure 1 shows both the top (a) and the cross-sectional view (b) of the free-standing film, revealing the horizontal alignment of the nanosheets in the stack.

APT Specimen Preparation

A first batch of needle-shaped APT specimens was prepared from the free-standing MXene film according to the lift-out and sharpening protocol introduced by Thompson et al. (2007), using a dual beam SEM-FIB (Helios Nanolab 600, FEI) equipped with a Ga ion source, as illustrated in Figure 2 (a) - (d). For a second batch of samples, the

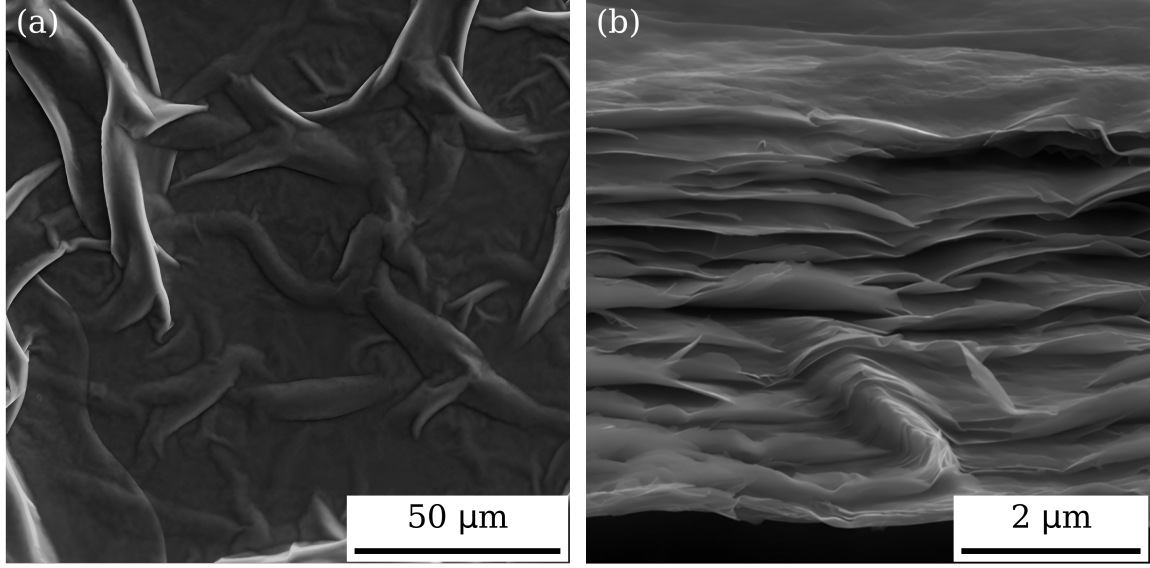


Figure 1: (a) Top and (b) cross-sectional view of the free-standing $\text{Ti}_3\text{C}_2\text{T}_x$ MXene film.

lift-out was first attached to a needle able to rotate the lifted-out lamella by 90° , thereby aligning the MXene nanosheets more favourably for APT analysis, and then picked up again with the micromanipulator to continue with common specimen preparation. After annular ion milling, specimens such as in Figure 3 (a) were then additionally coated with Cr (99.9 %, small leftover of the synthesis of larger ingots from the workshop at the Max-Planck-Institut für Eisenforschung) using an *in situ* sputtering technique described by Woods et al. (2023), building on previous reported works (Douglas et al. 2023; Kölling et al. 2009), and as depicted in Figure 3 (b). More details on the complete coating workflow can be found in Schwarz et al. (2023). Sputtering parameters for the ion beam pattern were 30 kV and 48 pA for 20 s to 30 s, repeated 4 times after rotating the specimen 90° each time to ensure a uniform coating. Cr as a coating material was chosen in first place for its well-known adhesion properties.

APT Characterization

APT analyses were performed using either a 5000XS (straight flight path) or a 5000XR (reflectron-fitted) local electrode atom probe (Cameca Instruments), operating in ultraviolet ($\lambda = 355$ nm) laser-pulsing mode. Parameters were set to a base temperature of 50 K, a laser pulse energy varied between 50 pJ and 75 pJ, a laser pulsing rate of 125 kHz, and a target detection rate of 5 to 10 ions per 1000 pulses on average. Data reconstruction and analysis was done with AP Suite 6.3 by Cameca Instruments following the default voltage-based reconstruction algorithm.

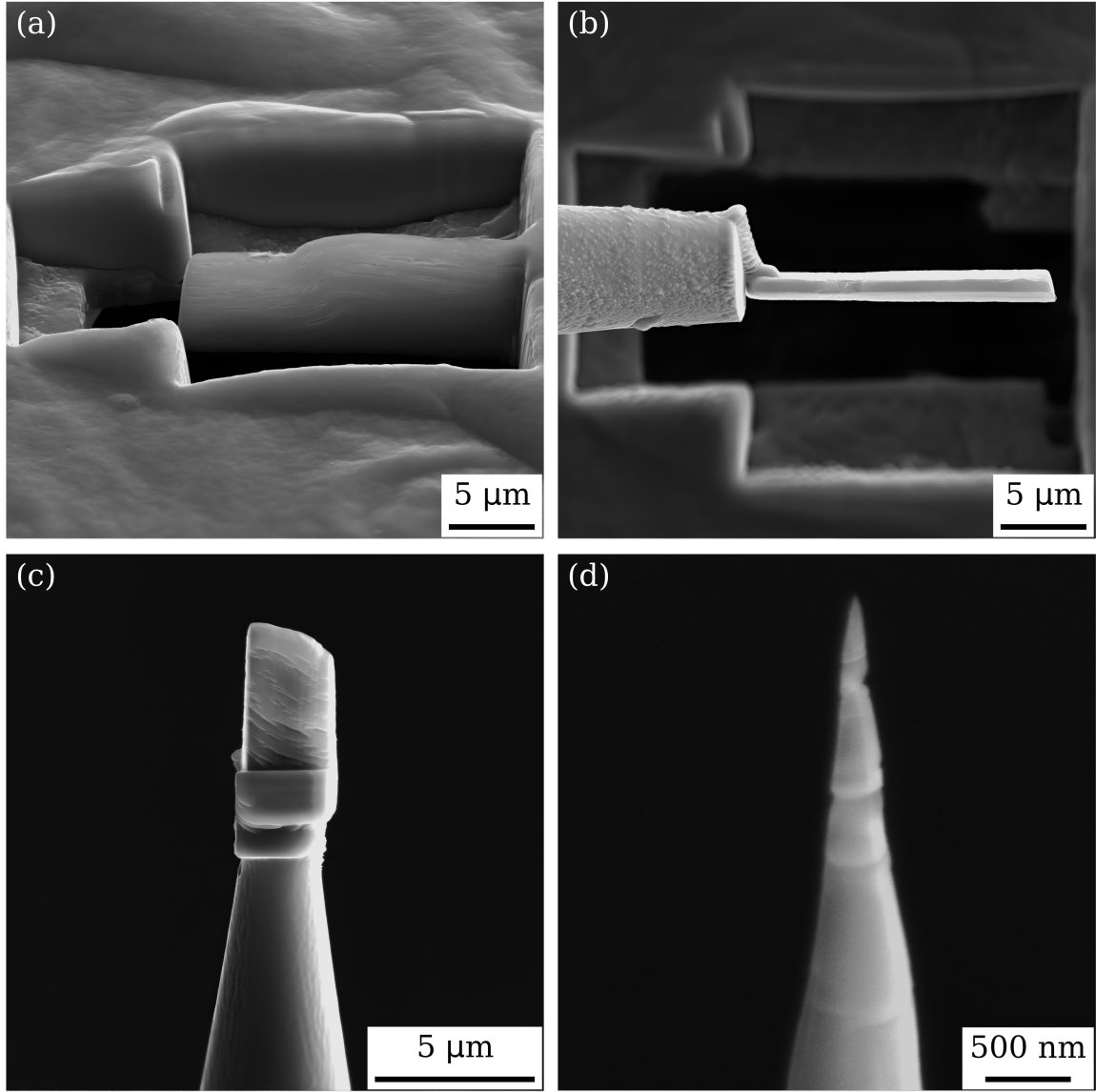


Figure 2: APT specimen preparation of the free-standing $\text{Ti}_3\text{C}_2\text{T}_x$ MXene film following common lift-out and sharpening protocols. (a) Cross-sectional view of a lamella sliced out of the film using the Ga ion beam. (b) Lift-out of the lamella, which is attached to a micromanipulator by decomposing a gaseous Pt/C precursor from a gas-injection system. (c) Mounted lift-out on a commercial silicon support. (d) Final sharpened APT specimen after annular ion milling. The horizontal stacking orientation of the nanosheets is readily visible.

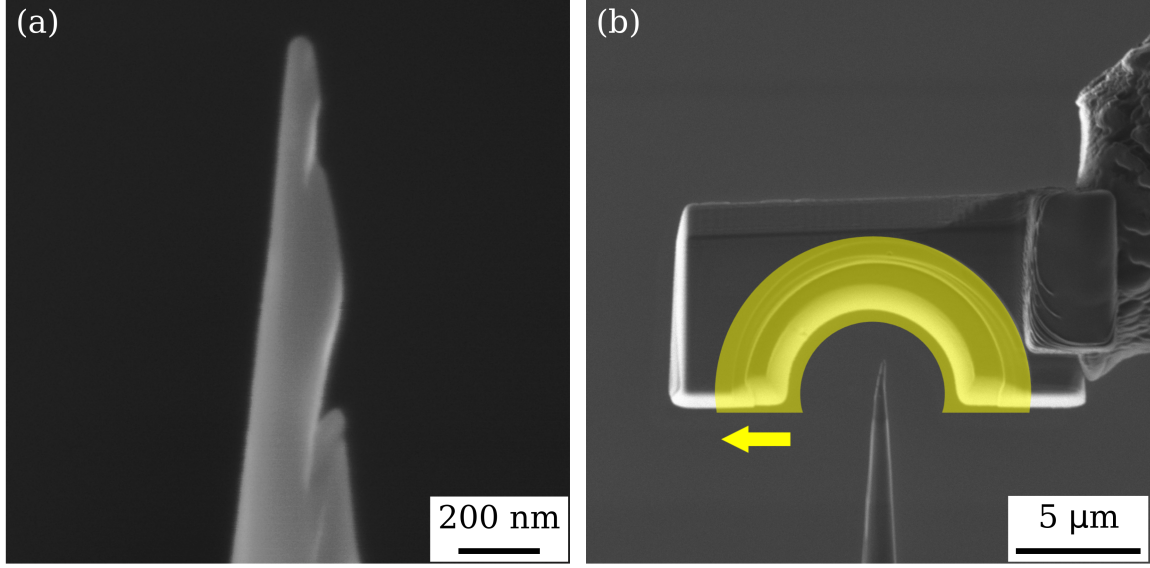


Figure 3: Revised APT specimen preparation for the free-standing $\text{Ti}_3\text{C}_2\text{T}_x$ MXene film utilizing the *in situ* sputtering technique. (a) Uncoated APT specimen. The lift-out was rotated to orient the nanosheets along the specimen. (b) *In situ* coating procedure. The milling pattern is schematically shown in yellow.

Results and Discussion

Mechanical Instability and *In Situ* Delithiation

Initial attempts to analyze APT specimens of the free-standing MXene film, prepared as described in Figure 4, faced significant problems with the mechanical stability of the specimens, that may be inherent in the APT analysis of such materials. In this arrangement, the stacking orientation of the nanosheets is perpendicular to the main axis of the APT specimen, as visible in Figure 2 (d). Despite the intermolecular interactions between the MXenes nanosheets, they are not strong enough to withstand the high Maxwell stresses arising from the intense electrostatic field applied during the analysis. In addition, there may also be nanovoids between the nanosheets, as visible in the cross-sectional view of the free-standing film in Figure 1 (b), where intermolecular forces will be almost absent. This results in multiple small fractures, as evidenced by drops in the base voltage curve in Figure 4 (a), which can be explained by a sudden increase in the detection rate due to the detection of several nanosheets breaking off from the specimen apex in very close succession. In almost all cases, measurements are limited to less than a million ions detected before the specimens fractures completely from the silicon support, so the success rate for these samples is rather low.

Li was normally only used in the wet chemical synthesis for exfoliation. However, here up to 90 at.% Li was measured in the analyzed specimens. In the reconstructed 3D atom map in Figure 4 (b), it was observed that at the beginning and after each microfracture, Li field evaporates first before other species such as Ti are also detected.

During APT analysis, the intense electrostatic field can cause preferential migration of Li atoms (Greiwe et al. 2014), also known as *in situ* delithiation (Pfeiffer et al. 2017), which is a known artifact in the analysis of Li-containing materials. Hot spots in the detector map in Figure 4 (c), localized preferentially on the side of the specimen directly illuminated by the laser, are another indicator for this phenomenon, since the temperature rise of the specimen due to the absorbed laser energy increases the mobility and thus the migration of the Li atoms (Kim et al. 2022a). Considering the observed mechanical instability of the specimen, the *in situ* delithiation could possibly even favor it, since the sudden deintercalation of Li may weaken the intermolecular forces between the nanosheets.

In summary, it was not possible to perform a reliable APT analysis on specimens of the free-standing 2D material film prepared using the common FIB lift-out and sharpening protocols. On the one hand, the specimens lack mechanical stability, and on the other hand, preferential migration of Li atoms prevents detailed compositional analysis.

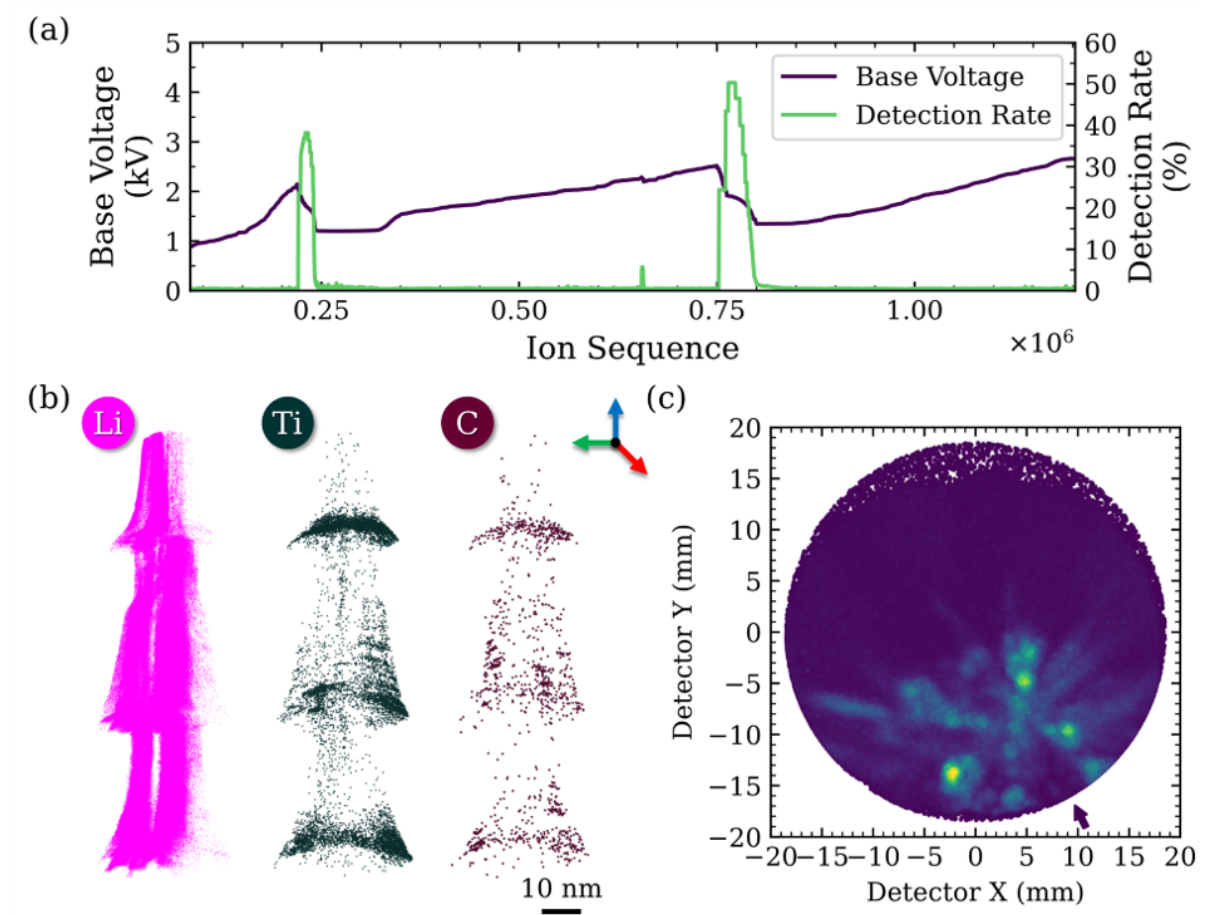


Figure 4: Characteristic APT analysis of the free-standing MXene film prepared following common lift-out and sharpening protocols. (a) Base voltage and detection rate curve. (b) Reconstructed 3D atom maps. (c) Detector hit map. The direction of the laser beam is indicated by an arrow.

***In Situ* Coating for Mechanical Stabilization**

In order to overcome both the mechanical instability and *in situ* delithiation issue that hinder successful APT analysis of the free-standing $\text{Ti}_3\text{C}_2\text{T}_z$ MXene film, specimens were prepared according to the workflow described in Figure 3. Coating of APT specimens resulted in enhanced yield for a wide range of materials (Kölling et al. 2009; Larson et al. 2013; Schwarz et al. 2023), for example by smoothing out the roughness of the specimen surface, but also suppressed *in situ* delithiation in battery materials (Kim et al. 2022a; Singh et al. n.d.), or the piezoelectric effect in perovskite-structured materials (Kim et al. 2023) by shielding the electrostatic field. By sputtering a material onto the specimen, pores and nanovoids may also be filled, which helps to reduce varying magnification in the reconstruction due to ion trajectory aberrations as well as possible crack tips for premature fracture during analysis (Pfeiffer et al. 2015). Various methods have been proposed to eliminate pores in APT specimens, such as electron beam induced deposition (Barroo et al. 2020; Pfeiffer et al. 2015), electrodeposition (Mouton et al. 2017; El-Zoka et al. 2017), liquid metal encapsulation (Kim et al. 2022b) or resin impregnation (Zand et al. 2023). However, these potential solutions have all their own drawbacks, such as exposing the material to an electrochemical environment, heat, or high pressure, which could alter the chemistry or structure of the material. *In situ* coating, on the other hand, has the advantage that a variety of materials can be used as sputter targets (Schwarz et al. 2023), and it can even be performed at cryogenic temperatures (Woods et al. 2023), minimizing the potential impact on the chemistry and structure of the material.

After metallic coating using the *in situ* sputtering technique, specimens of the free-standing MXene film were successfully analyzed by APT. As visible in the cross-section of the reconstructed 3D atom map in Figure 5 (b), the as-prepared free-standing MXene film specimen is well coated by Cr. Some of the Cr coating also seems to have penetrated into the stacked material, and has filled nanovoids between the nanosheets. Figure 5 (a) provides a plot of the base voltage and the background level curve of these data, both metrics that indicate how stable the measurement was. Except for small drops, the base voltage steadily and smoothly increases, indicating stable field evaporation conditions. The background is largely constant and below 10 ppm ns^{-1} on average. Previous studies have shown that a low and constant background level is essential for the detailed quantification of alkali elements such as Li (Kim et al. 2022a; Lu et al. 2017; Santhanagopalan et al. 2015), which can be lost in the background from uncorrelated DC field evaporation due to their low expected evaporation field compared to the other elements composing the material (Tsong 1978).

Compared to previous work, where exfoliated $\text{Ti}_3\text{C}_2\text{T}_z$ MXenes were electrodeposited into Co (Krämer et al. n.d.), significantly larger volumes of the material of interest were measured. To illustrate the improvement, the detected Ti ion counts, including the contribution of decomposed molecular ions, from the APT data of the exfoliated MXenes from Krämer et al. (n.d.) and the free-standing MXenes films were compared. While less than 0.1 million Ti ions were detected in the data set for the exfoliated MXenes embedded in Co, between 1.5 and 2 million Ti ions were collected in the free-standing MXene film in different measurements. All these values refer to data acquired on a 5000XR

instrument with a detection efficiency of 0.52 %. Notwithstanding the much simpler and time-saving specimen preparation workflow, the APT data obtained for the nanomaterial is significantly larger and therefore statistically more reliable. In addition, the detector hit maps of the Cr coated samples in Figure 5 (c) do not show characteristic hot spots, that would indicate a preferential migration of Li atoms. This confirms that the Cr coating prevents the *in situ* delithiation, as was suggested in previous studies (Singh et al. n.d.).

Besides Cr, other materials may also be considered as sputter targets in the future. Although it has been shown that specimens can be easily coated with Cr using the *in situ* sputtering technique, it has some disadvantages for this particular case. During the sputtering process, the clean Cr layer is constantly passivated with an oxide layer (Schwarz et al. 2023), despite the vacuum inside the SEM-FIB. Since the coating also penetrates into the free-standing film specimen itself to fill nanovoids, the detailed determination of the oxygen content of the nanomaterial becomes nearly impossible. Therefore, Cr should be replaced as coating material by a more chemically inert metal in further studies, depending on the adhesion and the probability of peak overlap with the material of interest in the APT mass spectrum.

Conclusion

Despite the great interest in understanding the functional properties of nanomaterials by characterizing their detailed composition, 2D materials have rarely been studied using APT. Using $\text{Ti}_3\text{C}_2\text{T}_z$ MXenes as an example, the common SEM-FIB specimen preparation has been revised utilizing an *in situ* sputtering technique to facilitate the APT analysis of 2D materials. By processing the colloidal MXene solution into an additive-free free-standing film to enable a common lift-out and sharpening procedure, and by coating the APT specimen, it was possible to acquire relatively large volumes of the 2D material with high data quality. The coating stabilizes the fragile specimen, but also prevents the *in situ* delithiation of Li, which was incorporated into the material during synthesis. As materials other than MXenes can also be processed into free-standing films (Dikin et al. 2007; Z. Li et al. 2023), the presented workflow has the potential to be a starting point to study the detailed composition of 2D materials with APT.

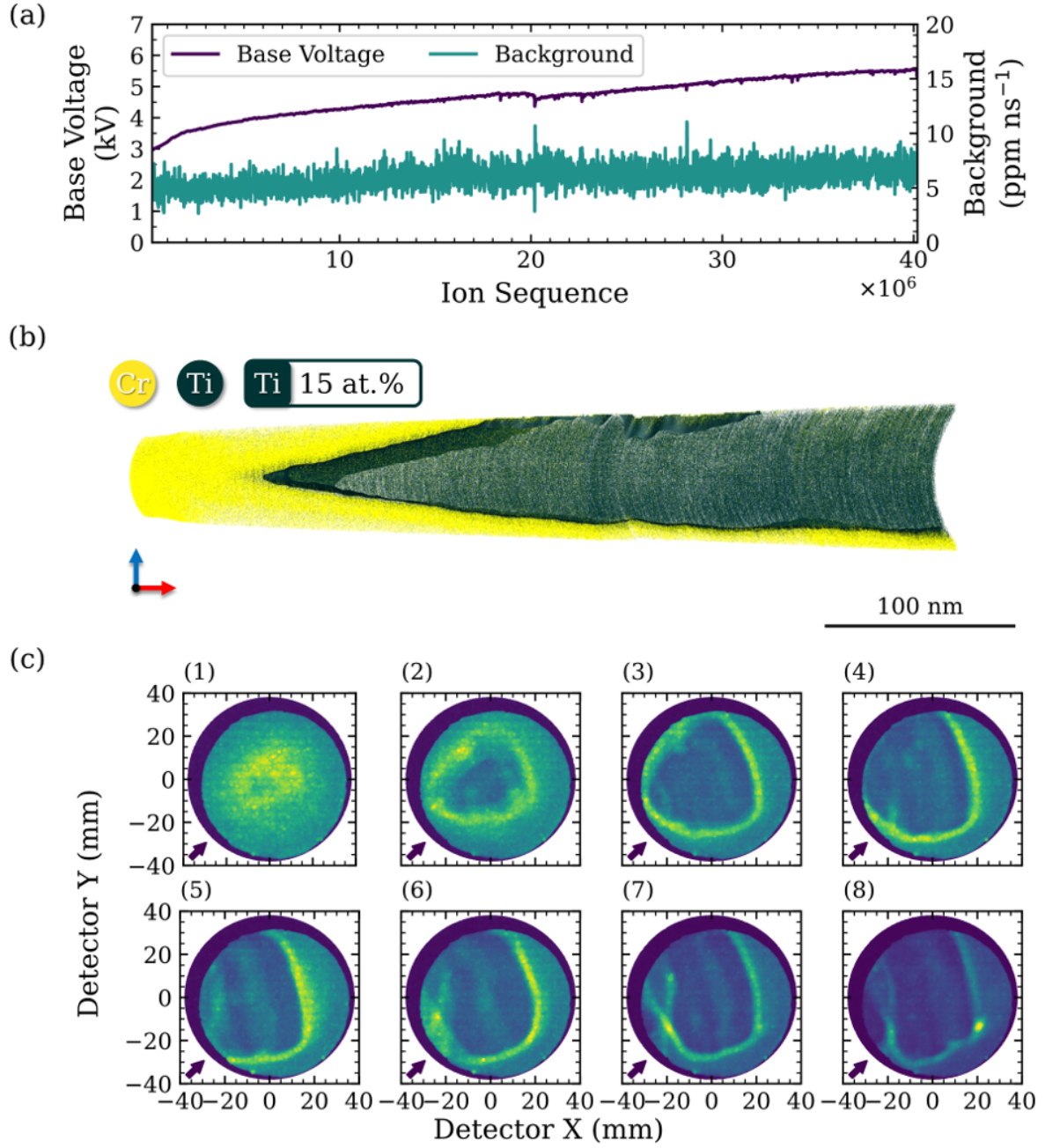


Figure 5: Characteristic APT analysis of the free-standing MXene film prepared following the revised specimen preparation. (a) Base voltage and background level curve. (b) Cross-section of the reconstructed 3D atom map. (c) History of the detector hit map during the measurement, starting at (1). The direction of the laser beam is indicated by an arrow.

Acknowledgment

The authors acknowledge financial support from the German Research Foundation (DFG) through DIP Project No. 450800666. The support to the FIB and APT facilities at MPIE by Uwe Tezins, Andreas Sturm and Christian Broß is gratefully acknowledged.

Conflict of Interest

The authors declare no conflict of interest.

Data Availability Statement

The data that support the findings of this study are available from the corresponding authors upon reasonable request.

References

- Adineh, Vahid R., Changxi Zheng, Qianhui Zhang, Ross K. W. Marceau, Boyin Liu, Yu Chen, Kae J. Si, Matthew Weyland, Tony Velkov, Wenlong Cheng, Jian Li, and Jing Fu (2018). "Graphene-Enhanced 3D Chemical Mapping of Biological Specimens at Near-Atomic Resolution." In: *Advanced Functional Materials* 28.32, p. 1801439. DOI: 10.1002/adfm.201801439.
- Alhabeb, Mohamed, Kathleen Maleski, Babak Anasori, Pavel Lelyukh, Leah Clark, Saleesha Sin, and Yury Gogotsi (2017). "Guidelines for Synthesis and Processing of Two-Dimensional Titanium Carbide (Ti₃C₂T_x MXene)." In: *Chemistry of Materials* 29.18, pp. 7633–7644. DOI: 10.1021/acs.chemmater.7b02847.
- Anasori, Babak, Michael Naguib, and Guest Editors (2023). "Two-dimensional MXenes." In: *MRS Bulletin* 48.3, pp. 238–244. DOI: 10.1557/s43577-023-00500-z.
- Barroo, Cédric, Austin J. Akey, and David C. Bell (2020). "Aggregated nanoparticles: Sample preparation and analysis by atom probe tomography." In: *Ultramicroscopy* 218, p. 113082. DOI: 10.1016/j.ultramicro.2020.113082.
- Chen, Hongwu, Yeye Wen, Yingyi Qi, Qian Zhao, Liangti Qu, and Chun Li (2020). "Pristine Titanium Carbide MXene Films with Environmentally Stable Conductivity and Superior Mechanical Strength." In: *Advanced Functional Materials* 30.5, p. 1906996. DOI: 10.1002/adfm.201906996.
- De Geuser, Frédéric and Baptiste Gault (2020). "Metrology of small particles and solute clusters by atom probe tomography." In: *Acta Materialia* 188, pp. 406–415. DOI: 10.1016/j.actamat.2020.02.023.
- Devaraj, A., M. Gu, R. Colby, P. Yan, C. M. Wang, J. M. Zheng, J. Xiao, A. Genc, J. G. Zhang, I. Belharouak, D. Wang, K. Amine, and S. Thevuthasan (2015). "Visualizing nanoscale 3D compositional fluctuation of lithium in advanced lithium-ion battery cathodes." In: *Nature Communications* 6.1, p. 8014. DOI: 10.1038/ncomms9014.

- Dikin, Dmitriy A., Sasha Stankovich, Eric J. Zimney, Richard D. Piner, Geoffrey H. B. Dommett, Guennadi Evmenenko, SonBinh T. Nguyen, and Rodney S. Ruoff (2007). "Preparation and characterization of graphene oxide paper." In: *Nature* 448.7152, pp. 457–460. DOI: 10.1038/nature06016.
- Douglas, James O, Michele Conroy, Finn Giuliani, and Baptiste Gault (2023). "In Situ Sputtering From the Micromanipulator to Enable Cryogenic Preparation of Specimens for Atom Probe Tomography by Focused-Ion Beam." In: *Microscopy and Microanalysis* 29.3, pp. 1009–1017. DOI: 10.1093/micmic/ozad020.
- Du, Sichao, Timothy Burgess, Shyeh Tjing Loi, Baptiste Gault, Qiang Gao, Peite Bao, Li Li, Xiangyuan Cui, Wai Kong Yeoh, Hark Hoe Tan, Chennupati Jagadish, Simon P. Ringer, and Rongkun Zheng (2013). "Full tip imaging in atom probe tomography." In: *Ultramicroscopy* 124, pp. 96–101. DOI: 10.1016/j.ultramic.2012.08.014.
- Felfer, P., T. Li, K. Eder, H. Galinski, A.P. Magyar, D.C. Bell, G.D.W. Smith, N. Kruse, S.P. Ringer, and J.M. Cairney (2015). "New approaches to nanoparticle sample fabrication for atom probe tomography." In: *Ultramicroscopy* 159, pp. 413–419. DOI: 10.1016/j.ultramic.2015.04.014.
- Gault, Baptiste, Ann Chiaramonti, Oana Cojocaru-Mirédin, Patrick Stender, Renelle Dubosq, Christoph Freysoldt, Surendra Kumar Makineni, Tong Li, Michael Moody, and Julie M. Cairney (2021). "Atom probe tomography." In: *Nature Reviews Methods Primers* 1.1, p. 51. DOI: 10.1038/s43586-021-00047-w.
- Ghidiu, Michael, Maria R. Lukatskaya, Meng-Qiang Zhao, Yury Gogotsi, and Michel W. Barsoum (2014). "Conductive two-dimensional titanium carbide 'clay' with high volumetric capacitance." In: *Nature* 516.7529, pp. 78–81. DOI: 10.1038/nature13970.
- Greiwe, Gerd-Hendrik, Zoltan Balogh, and Guido Schmitz (2014). "Atom probe tomography of lithium-doped network glasses." In: *Ultramicroscopy* 141, pp. 51–55. DOI: 10.1016/j.ultramic.2014.03.007.
- Josten, Jan P and Peter J Felfer (2022). "Atom Probe Analysis of Nanoparticles Through Pick and Coat Sample Preparation." In: *Microscopy and Microanalysis* 28.4, pp. 1188–1197. DOI: 10.1017/S1431927621000465.
- Kim, Se-Ho, Stoichko Antonov, Xuyang Zhou, Leigh T. Stephenson, Chanwon Jung, Ayman A. El-Zoka, Daniel K. Schreiber, Michele Conroy, and Baptiste Gault (2022a). "Atom probe analysis of electrode materials for Li-ion batteries: challenges and ways forward." In: *Journal of Materials Chemistry A* 10 (9), pp. 4926–4935. DOI: 10.1039/D1TA10050E.
- Kim, Se-Ho, Phil Woong Kang, O Ok Park, Jae-Bok Seol, Jae-Pyoung Ahn, Ji Yeong Lee, and Pyuck-Pa Choi (2018). "A new method for mapping the three-dimensional atomic distribution within nanoparticles by atom probe tomography (APT)." In: *Ultramicroscopy* 190, pp. 30–38. DOI: 10.1016/j.ultramic.2018.04.005.
- Kim, Se-Ho, Joohyun Lim, Rajib Sahu, Olga Kasian, Leigh T. Stephenson, Christina Scheu, and Baptiste Gault (2020). "Direct Imaging of Dopant and Impurity Distributions in 2D MoS₂." In: *Advanced Materials* 32.8, p. 1907235. DOI: 10.1002/adma.201907235.
- Kim, Se-Ho, Kihyun Shin, Xuyang Zhou, Chanwon Jung, Hyun You Kim, Stella Pedrazzini, Michele Conroy, Graeme Henkelman, and Baptiste Gault (2023). "Atom probe analysis

- of BaTiO₃ enabled by metallic shielding.” In: *Scripta Materialia* 229, p. 115370. DOI: 10.1016/j.scriptamat.2023.115370.
- Kim, Se-Ho, Ayman A. El-Zoka, and Baptiste Gault (2022b). “A Liquid Metal Encapsulation for Analyzing Porous Nanomaterials by Atom Probe Tomography.” In: *Microscopy and Microanalysis* 28.4, pp. 1198–1206. DOI: 10.1017/S1431927621012964.
- Kölling, S. and W. Vandervorst (2009). “Failure mechanisms of silicon-based atom-probe tips.” In: *Ultramicroscopy* 109.5, pp. 486–491. DOI: 10.1016/j.ultramicro.2008.11.013.
- Krämer, Mathias, Bar Favelukis, Ayman A. El-Zoka, Maxim Sokol, Brian A. Rosen, Noam Eliaz, Se-Ho Kim, and Baptiste Gault (n.d.). “Near-Atomic Scale Perspective on the Oxidation of Ti₃C₂T_x MXenes: Insights from Atom Probe Tomography.” In: *Advanced Materials* n/a.n/a (), p. 2305183. DOI: 10.1002/adma.202305183.
- Lan, Changyong, Ziyao Zhou, Renjie Wei, and Johnny C. Ho (2019). “Two-dimensional perovskite materials: From synthesis to energy-related applications.” In: *Materials Today Energy* 11, pp. 61–82. DOI: 10.1016/j.mtener.2018.10.008.
- Larson, D.J., A.D. Giddings, Y. Wu, M.A. Verheijen, T.J. Prosa, F. Roozeboom, K.P. Rice, W.M.M. Kessels, B.P. Geiser, and T.F. Kelly (2015). “Encapsulation method for atom probe tomography analysis of nanoparticles.” In: *Ultramicroscopy* 159, pp. 420–426. DOI: 10.1016/j.ultramicro.2015.02.014.
- Larson, D.J., T.J. Prosa, J.H. Bunton, D.P. Olson, D.F. Lawrence, E. Oltman, S.N. Strennin, and T.F. Kelly (2013). “Improved Mass Resolving Power and Yield in Atom Probe Tomography.” In: *Microscopy and Microanalysis* 19.S2, pp. 994–995. DOI: 10.1017/S143192761300696X.
- Li, Tong, Arun Devaraj, and Norbert Kruse (2022). “Atomic-scale characterization of (electro-)catalysts and battery materials by atom probe tomography.” In: *Cell Reports Physical Science* 3.12, p. 101188. DOI: 10.1016/j.xcrp.2022.101188.
- Li, Xiuyan and K. Lu (2017). “Playing with defects in metals.” In: *Nature Materials* 16.7, pp. 700–701. DOI: 10.1038/nmat4929.
- Li, Zhuangnan, Ismail Sami, Jieun Yang, Juntao Li, Ramachandran Vasant Kumar, and Manish Chhowalla (2023). “Lithiated metallic molybdenum disulfide nanosheets for high-performance lithium–sulfur batteries.” In: *Nature Energy* 8.1, pp. 84–93. DOI: 10.1038/s41560-022-01175-7.
- Lim, Kang Rui Garrick, Mikhail Shekhiriev, Brian C. Wyatt, Babak Anasori, Yury Gogotsi, and Zhi Wei Seh (2022). “Fundamentals of MXene synthesis.” In: *Nature Synthesis* 1.8, pp. 601–614. DOI: 10.1038/s44160-022-00104-6.
- Lipatov, Alexey, Mohamed Alhabeb, Maria R. Lukatskaya, Alex Boson, Yury Gogotsi, and Alexander Sinitskii (2016). “Effect of Synthesis on Quality, Electronic Properties and Environmental Stability of Individual Monolayer Ti₃C₂ MXene Flakes.” In: *Advanced Electronic Materials* 2.12, p. 1600255. DOI: 10.1002/aelm.201600255.
- Lu, Xiaonan, Daniel K. Schreiber, James J. Neeway, Joseph V. Ryan, and Jincheng Du (2017). “Effects of optical dopants and laser wavelength on atom probe tomography analyses of borosilicate glasses.” In: *Journal of the American Ceramic Society* 100.10, pp. 4801–4815. DOI: 10.1111/jace.14987.

- Lukatskaya, Maria R., Olha Mashtalir, Chang E. Ren, Yohan Dall’Agnese, Patrick Rozier, Pierre Louis Taberna, Michael Naguib, Patrice Simon, Michel W. Barsoum, and Yury Gogotsi (2013). “Cation Intercalation and High Volumetric Capacitance of Two-Dimensional Titanium Carbide.” In: *Science* 341.6153, pp. 1502–1505. DOI: 10.1126/science.1241488.
- Mannix, Andrew J., Brian Kiraly, Mark C. Hersam, and Nathan P. Guisinger (2017). “Synthesis and chemistry of elemental 2D materials.” In: *Nature Reviews Chemistry* 1.2, p. 0014. DOI: 10.1038/s41570-016-0014.
- Manzeli, Sajede, Dmitry Ovchinnikov, Diego Pasquier, Oleg V. Yazyev, and Andras Kis (2017). “2D transition metal dichalcogenides.” In: *Nature Reviews Materials* 2.8, p. 17033. DOI: 10.1038/natrevmats.2017.33.
- Mouton, Isabelle, Tony Printemps, Adeline Grenier, Narciso Gambacorti, Elisa Pinna, Mariavitalia Tiddia, Annalisa Vacca, and Guido Mula (2017). “Toward an accurate quantification in atom probe tomography reconstruction by correlative electron tomography approach on nanoporous materials.” In: *Ultramicroscopy* 182, pp. 112–117. DOI: 10.1016/j.ultramic.2017.06.007.
- Naguib, Michael, Murat Kurtoglu, Volker Presser, Jun Lu, Junjie Niu, Min Heon, Lars Hultman, Yury Gogotsi, and Michel W. Barsoum (2011). “Two-Dimensional Nanocrystals Produced by Exfoliation of Ti_3AlC_2 .” In: *Advanced Materials* 23.37, pp. 4248–4253. DOI: 10.1002/adma.201102306.
- Nicolosi, Valeria, Manish Chhowalla, Mercouri G. Kanatzidis, Michael S. Strano, and Jonathan N. Coleman (2013). “Liquid Exfoliation of Layered Materials.” In: *Science* 340.6139, p. 1226419. DOI: 10.1126/science.1226419.
- Novoselov, K. S., A. K. Geim, S. V. Morozov, D. Jiang, Y. Zhang, S. V. Dubonos, I. V. Grigorieva, and A. A. Firsov (2004). “Electric Field Effect in Atomically Thin Carbon Films.” In: *Science* 306.5696, pp. 666–669. DOI: 10.1126/science.1102896.
- Perea, Daniel E., Jonathan E. Allen, Steven J. May, Bruce W. Wessels, David N. Seidman, and Lincoln J. Lauhon (2006). “Three-Dimensional Nanoscale Composition Mapping of Semiconductor Nanowires.” In: *Nano Letters* 6.2, pp. 181–185. DOI: 10.1021/nl051602p.
- Pfeiffer, Björn, Torben Erichsen, Eike Epler, Cynthia A Volkert, Piet Trompenaars, and Carsten Nowak (2015). “Characterization of Nanoporous Materials with Atom Probe Tomography.” In: *Microscopy and Microanalysis* 21.3, pp. 557–563. DOI: 10.1017/S1431927615000501.
- Pfeiffer, Björn, Johannes Maier, Jonas Arlt, and Carsten Nowak (2017). “In Situ Atom Probe Deintercalation of Lithium-Manganese-Oxide.” In: *Microscopy and Microanalysis* 23.2, pp. 314–320. DOI: 10.1017/S1431927616012691.
- Qiu, Shi, Vivek Garg, Shuo Zhang, Yu Chen, Jian Li, Adam Taylor, Ross K.W. Marceau, and Jing Fu (2020a). “Graphene encapsulation enabled high-throughput atom probe tomography of liquid specimens.” In: *Ultramicroscopy* 216, p. 113036. DOI: 10.1016/j.ultramic.2020.113036.
- Qiu, Shi, Changxi Zheng, Vivek Garg, Yu Chen, Gediminas Gervinskas, Jian Li, Michelle A. Dunstone, Ross K. W. Marceau, and Jing Fu (2020b). “Three-Dimensional Chemical

- Mapping of a Single Protein in the Hydrated State with Atom Probe Tomography.” In: *Analytical Chemistry* 92.7, pp. 5168–5177. DOI: 10.1021/acs.analchem.9b05668.
- Qiu, Shi, Changxi Zheng, Qi Zhou, Dashen Dong, Qianqian Shi, Vivek Garg, Wenlong Cheng, Ross K.W. Marceau, Gang Sha, and Jing Fu (2020c). “Direct Imaging of Liquid–Nanoparticle Interfaces with Atom Probe Tomography.” In: *The Journal of Physical Chemistry C* 124.35, pp. 19389–19395. DOI: 10.1021/acs.jpcc.0c05504.
- Sang, Xiahan, Yu Xie, Ming-Wei Lin, Mohamed Alhabeb, Katherine L. Van Aken, Yury Gogotsi, Paul R. C. Kent, Kai Xiao, and Raymond R. Unocic (2016). “Atomic Defects in Monolayer Titanium Carbide (Ti₃C₂Tx) MXene.” In: *ACS Nano* 10.10, pp. 9193–9200. DOI: 10.1021/acsnano.6b05240.
- Santhanagopalan, Dhamodaran, Daniel K. Schreiber, Daniel E. Perea, Richard L. Martens, Yuri Janssen, Peter Khalifah, and Ying Shirley Meng (2015). “Effects of laser energy and wavelength on the analysis of LiFePO₄ using laser assisted atom probe tomography.” In: *Ultramicroscopy* 148, pp. 57–66. DOI: 10.1016/j.ultramicro.2014.09.004.
- Schwarz, Tim M., Eric Woods, Mahander P. Singh, Chanwon Jung, Leonardo S. Aota, Kyuseon Jang, Mathias Krämer, Se-Ho Kim, Ingrid McCarroll, and Baptiste Gault (2023). *In-situ metallic coating of atom probe specimen for enhanced yield, performance, and increased field-of-view*. arXiv: 2309.07836 [physics.app-ph].
- Shekhirev, Mikhail, Jeffrey Busa, Christopher E. Shuck, Angel Torres, Saman Bagheri, Alexander Sinitskii, and Yury Gogotsi (2022). “Ultralarge Flakes of Ti₃C₂Tx MXene via Soft Delamination.” In: *ACS Nano* 16.9, pp. 13695–13703. DOI: 10.1021/acsnano.2c04506.
- Shekhirev, Mikhail, Christopher E. Shuck, Asia Sarycheva, and Yury Gogotsi (2021). “Characterization of MXenes at every step, from their precursors to single flakes and assembled films.” In: *Progress in Materials Science* 120, p. 100757. DOI: 10.1016/j.pmatsci.2020.100757.
- Shuck, Christopher E. (2023). “MXenes are materials, not chemicals: Synthesis factors that influence MXene properties.” In: *MRS Communications*. DOI: 10.1557/s43579-023-00442-2.
- Shuck, Christopher E., Asia Sarycheva, Mark Anayee, Ariana Levitt, Yuanzhe Zhu, Simge Uzun, Vitaliy Balitskiy, Veronika Zahorodna, Oleksiy Gogotsi, and Yury Gogotsi (2020). “Scalable Synthesis of Ti₃C₂Tx MXene.” In: *Advanced Engineering Materials* 22.3, p. 1901241. DOI: 10.1002/adem.201901241.
- Singh, Mahander Pratap, Eric V Woods, Se-Ho Kim, Chanwon Jung, Leonardo S. Aota, and Baptiste Gault (n.d.). “Facilitating the systematic nanoscale study of battery materials by atom probe tomography through in-situ metal coating.” In: *Batteries & Supercaps* n/a.n/a (), e202300403. DOI: 10.1002/batt.202300403.
- Tedsree, Karaked, Tong Li, Simon Jones, Chun Wong Aaron Chan, Kai Man Kerry Yu, Paul A. J. Bagot, Emmanuelle A. Marquis, George D. W. Smith, and Shik Chi Edman Tsang (2011). “Hydrogen production from formic acid decomposition at room temperature using a Ag–Pd core–shell nanocatalyst.” In: *Nature Nanotechnology* 6.5, pp. 302–307. DOI: 10.1038/nnano.2011.42.
- Thakur, Anupma, Nithin Chandran B.S., Karis Davidson, Annabelle Bedford, Hui Fang, Yooran Im, Vaishnavi Kanduri, Brian C. Wyatt, Srinivasa Kartik Nemani, Valeriia

- Poliukhova, Ravi Kumar, Zahra Fakhraai, and Babak Anasori (2023). “Step-by-Step Guide for Synthesis and Delamination of Ti₃C₂Tx MXene.” In: *Small Methods* 7.8, p. 2300030. DOI: 10.1002/smtd.202300030.
- Thompson, K., D. Lawrence, D.J. Larson, J.D. Olson, T.F. Kelly, and B. Gorman (2007). “In situ site-specific specimen preparation for atom probe tomography.” In: *Ultramicroscopy* 107.2, pp. 131–139. DOI: 10.1016/j.ultramicro.2006.06.008.
- Tsong, T.T. (1978). “Field ion image formation.” In: *Surface Science* 70.1, pp. 211–233. DOI: 10.1016/0039-6028(78)90410-7.
- VahidMohammadi, Armin, Johanna Rosen, and Yury Gogotsi (2021). “The world of two-dimensional carbides and nitrides (MXenes).” In: *Science* 372.6547, eabf1581. DOI: 10.1126/science.abf1581.
- Woods, Eric V, Mahander P Singh, Se-Ho Kim, Tim M Schwarz, James O Douglas, Ayman A El-Zoka, Finn Giuliani, and Baptiste Gault (2023). “A Versatile and Reproducible Cryo-sample Preparation Methodology for Atom Probe Studies.” In: *Microscopy and Microanalysis*, ozad120. DOI: 10.1093/micmic/ozad120.
- Zand, Florian, Suzanne J. T. Hangx, Christopher J. Spiers, Peter J. van den Brink, James Burns, Matthew G. Boebinger, Jonathan D. Poplawsky, Matteo Monai, and Bert M. Weckhuysen (2023). “Elucidating the Structure and Composition of Individual Bimetallic Nanoparticles in Supported Catalysts by Atom Probe Tomography.” In: *Journal of the American Chemical Society* 145.31, pp. 17299–17308. DOI: 10.1021/jacs.3c04474.
- Zhang, Chuanfang (John), Lorcan McKeon, Matthias P. Kremer, Sang-Hoon Park, Oskar Ronan, Andrés Seral-Ascaso, Sebastian Barwich, Cormac Ó Coileáin, Niall McEvoy, Hannah C. Nerl, Babak Anasori, Jonathan N. Coleman, Yury Gogotsi, and Valeria Nicolosi (2019). “Additive-free MXene inks and direct printing of micro-supercapacitors.” In: *Nature Communications* 10.1, p. 1795. DOI: 10.1038/s41467-019-09398-1.
- Zhang, Jizhen, Na Kong, Simge Uzun, Ariana Levitt, Shayan Seyedin, Peter A. Lynch, Si Qin, Meikang Han, Wenrong Yang, Jingquan Liu, Xungai Wang, Yury Gogotsi, and Joselito M. Razal (2020). “Scalable Manufacturing of Free-Standing, Strong Ti₃C₂Tx MXene Films with Outstanding Conductivity.” In: *Advanced Materials* 32.23, p. 2001093. DOI: 10.1002/adma.202001093.
- El-Zoka, A.A., B. Langelier, G.A. Botton, and R.C. Newman (2017). “Enhanced analysis of nanoporous gold by atom probe tomography.” In: *Materials Characterization* 128, pp. 269–277. DOI: 10.1016/j.matchar.2017.03.013.